

Supporting Information

CO₂-Switchable amidine-modified ZIF-90 stabilized Pickering emulsions for controllable Knoevenagel condensation reaction

Xiaoyan Pei,^a Wangyue Song,^a Yang Zhao^b and Zhiyong Li^{*b}

^a*College of Chemistry and Chemical Engineering, Xinyang Normal University, Xinyang, Henan 464000, P. R. China.*

^b*Collaborative Innovation Center of Henan Province for Green Manufacturing of Fine Chemicals, Key Laboratory of Green Chemical Media and Reactions, Ministry of Education, School of Chemistry and Chemical Engineering, Henan Normal University, Xinxiang, Henan 453007, P. R. China.*

* Corresponding author

E-mail: yli@htu.edu.cn (**Zhiyong Li**)

Number of pages: 12

Number of figures: 26

Figures S1-S26

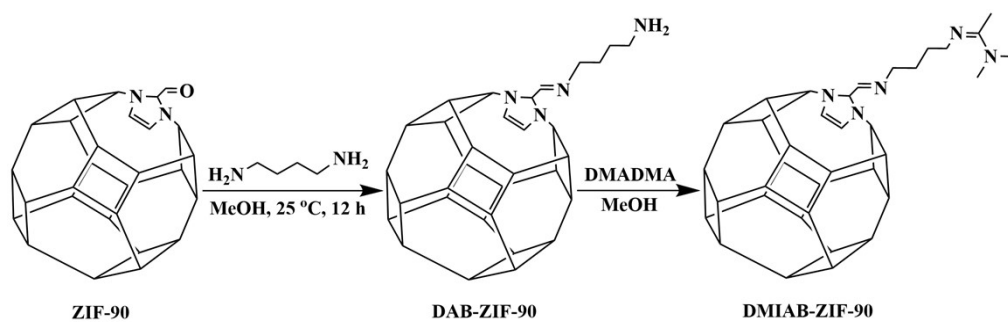


Figure S1 General procedure for the preparation of the amidine-modified ZIF-90.

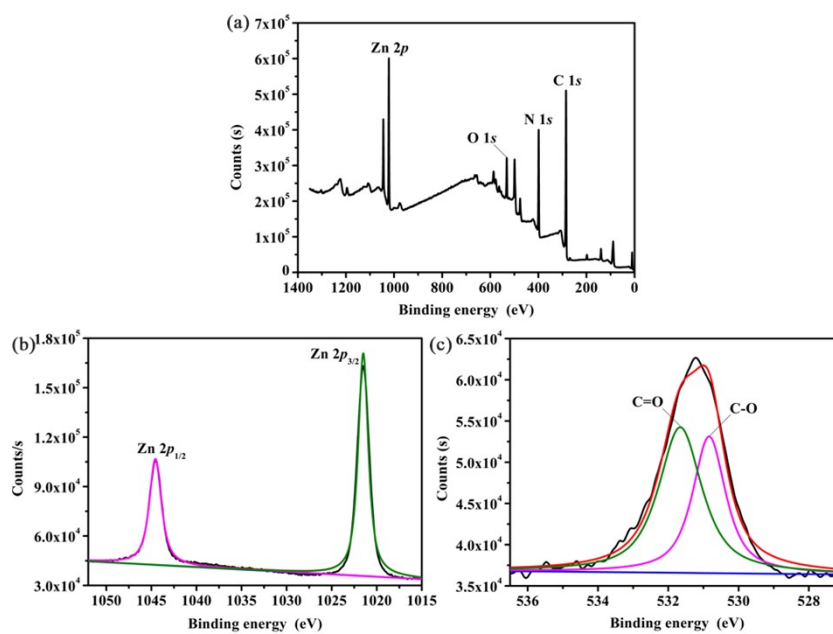


Figure S2 XPS spectra (a), high-resolution XPS spectra of N 1s (b) and O 1s (c) for DMIAB-ZIF-90.

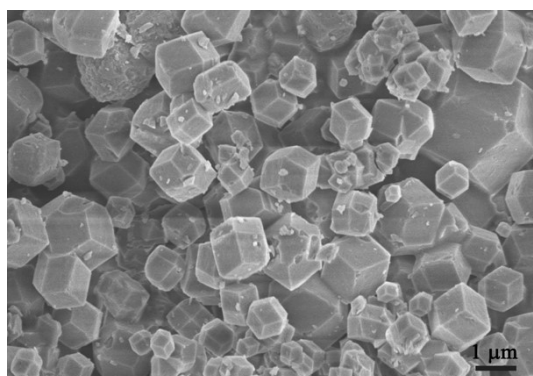


Figure S3 SEM image of the original ZIF-90.

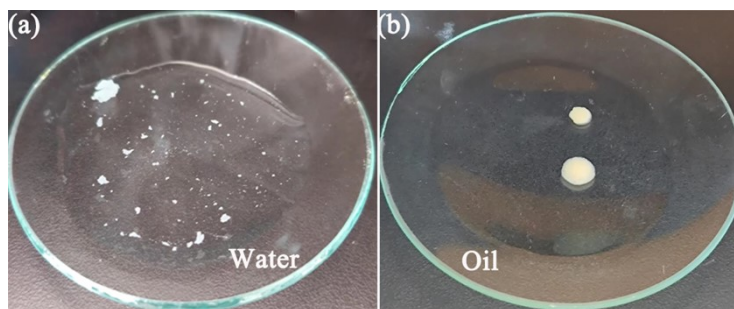


Figure S4 Photographs of the appearance of emulsion droplets in water and cyclohexane: (a) the DMIAB-ZIF-90-stabilized Pickering emulsion droplet dispersed in water, and (b) the emulsion droplet dispersed in cyclohexane.

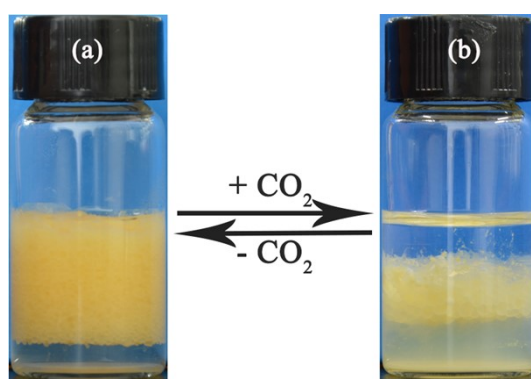


Figure S5 Photographs of the reversible switching between emulsification (a) and demulsification (b) of DMIAB-ZIF-90-stabilized Pickering emulsions ($V_{\text{benzene}}/V_{\text{water}} = 3:2$) driven by CO_2 .

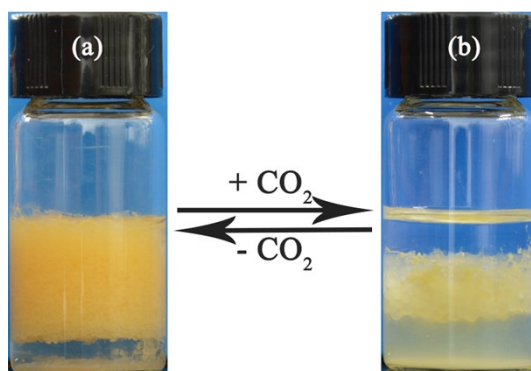


Figure S6 Photographs of the reversible switching between emulsification (a) and demulsification (b) of DMIAB-ZIF-90-stabilized Pickering emulsions ($V_{\text{toluene}}/V_{\text{water}} = 3:2$) driven by CO_2 .

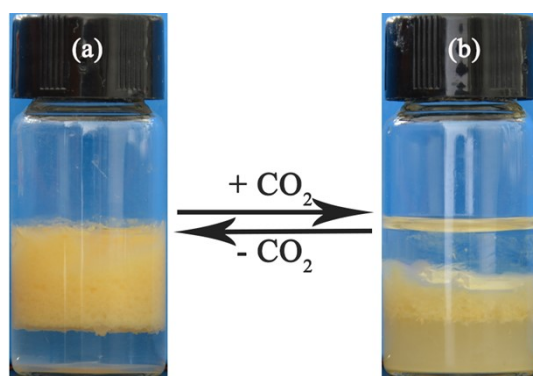


Figure S7 Photographs of the reversible switching between emulsification (a) and demulsification (b) of DMIAB-ZIF-90-stabilized Pickering emulsions ($V_{\text{n-hexane}}/V_{\text{water}} = 3: 2$) driven by CO_2 .

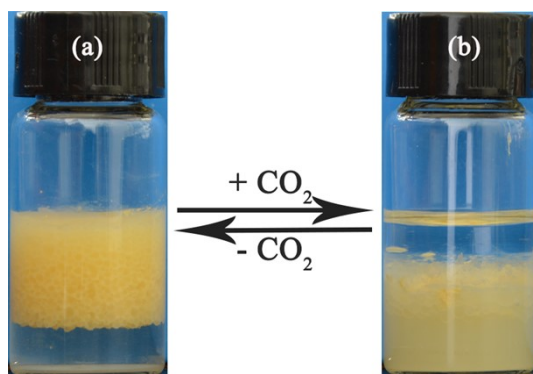


Figure S8 Photographs of the reversible switching between emulsification (a) and demulsification (b) of DMIAB-ZIF-90-stabilized Pickering emulsions ($V_{\text{n-heptane}}/V_{\text{water}} = 3: 2$) driven by CO_2 .

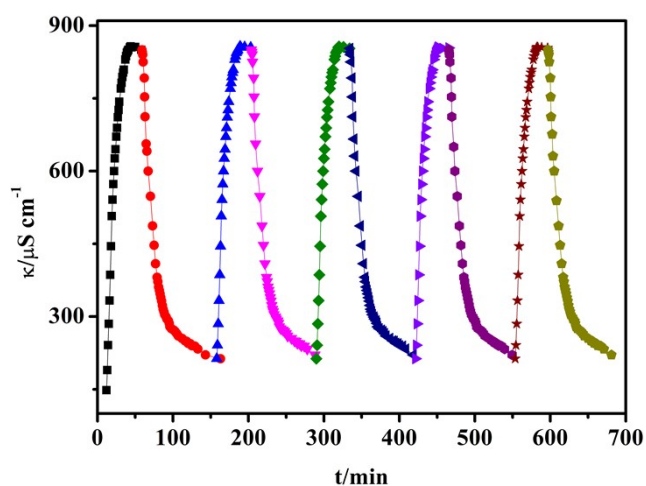


Figure S9 Conductivity of 1 wt% DMIAB-ZIF-90 dispersed in water as a function of time by alternating treatment with CO_2 and N_2 .

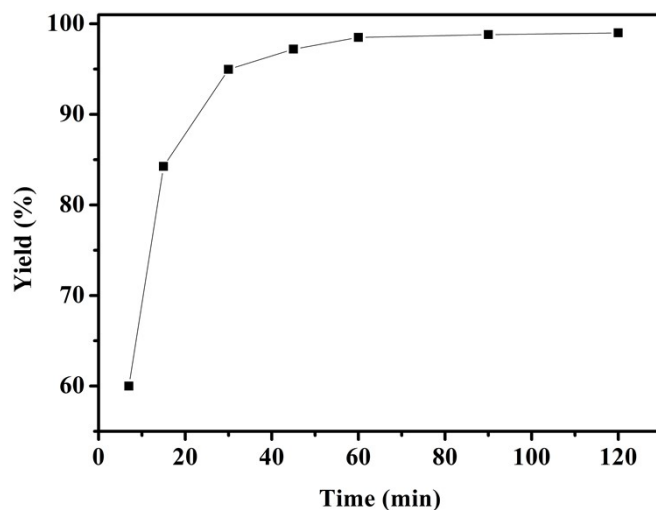


Figure S10 The variation of 2-benzylidenemalononitrile yield with reaction time in DMIAB-ZIF-90-based Pickering emulsion at 25 °C.

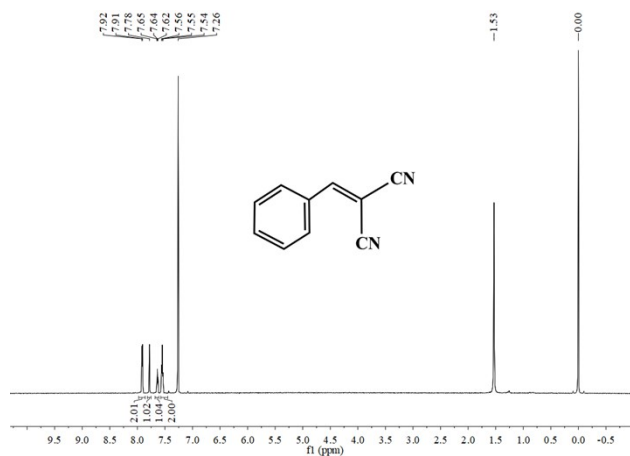


Figure S11 ^1H NMR spectra of 2-benzylidenemalononitrile.

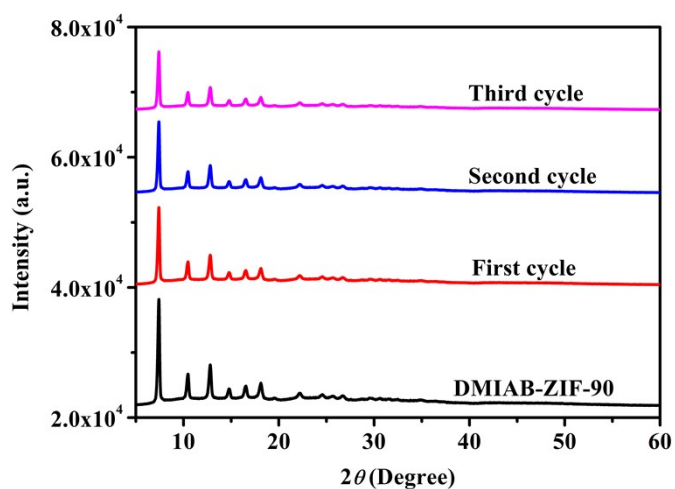


Figure S12 XRD patterns of DMIAB-ZIF-90 before and after each catalytic run.

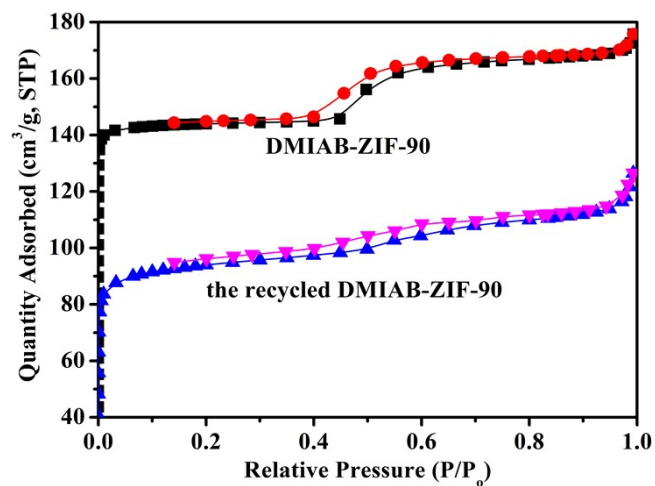


Figure S13 N_2 adsorption-desorption isotherms of DMIAB-ZIF-90 after three cycles of catalysis.

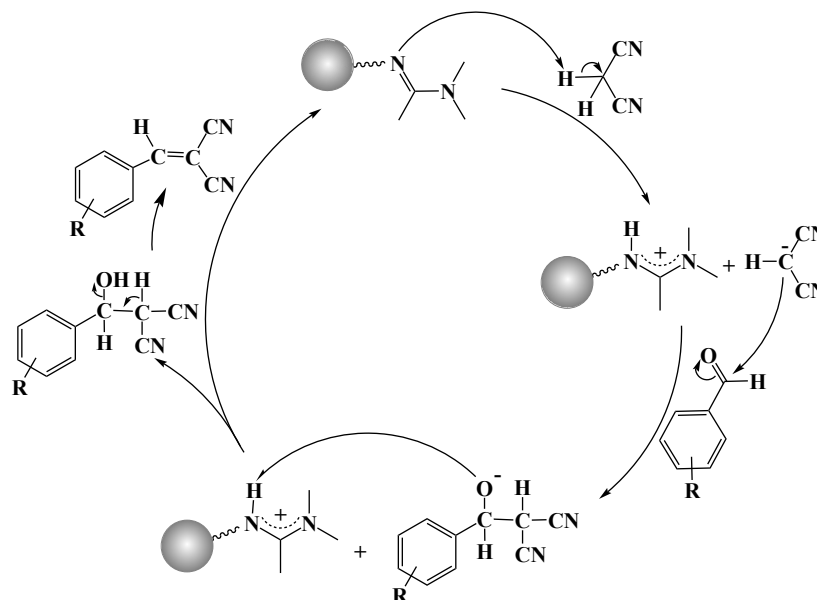


Figure S14 Proposed mechanism for the Knoevenagel condensation catalyzed by DMIAB-ZIF-90.

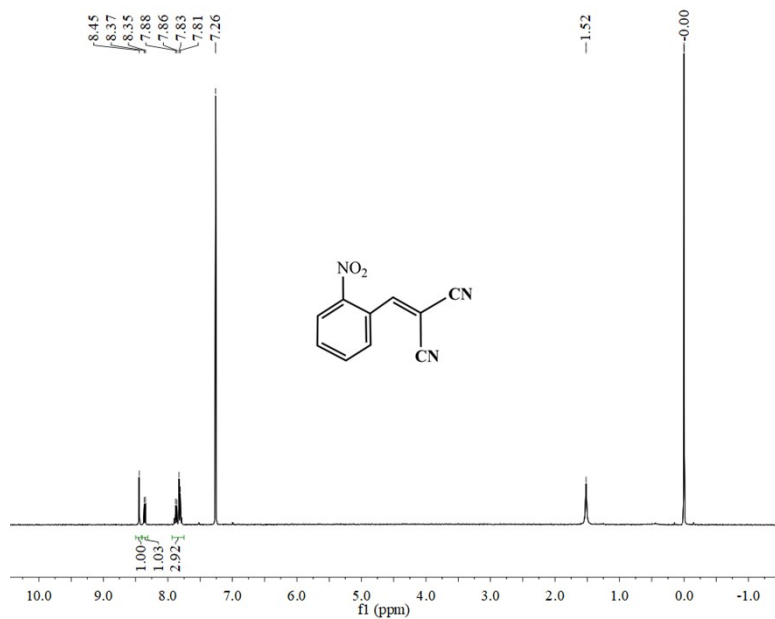


Figure S15 ^1H NMR spectra of 2-(2-nitrobenzylidene)malononitrile.

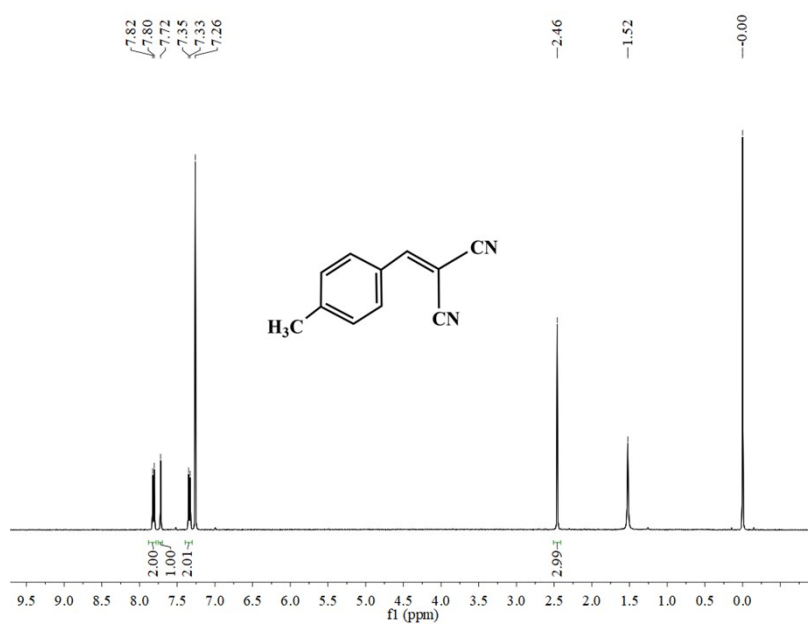


Figure S16 ^1H NMR spectra of 2-(4-methylbenzylidene)malononitrile.

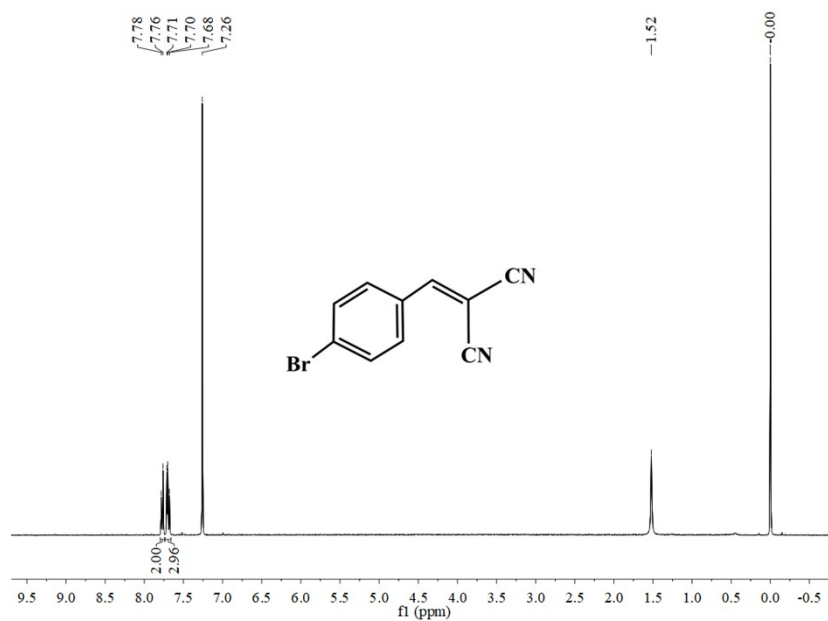


Figure S19 ^1H NMR spectra of 2-(4-bromobenzylidene)malononitrile.

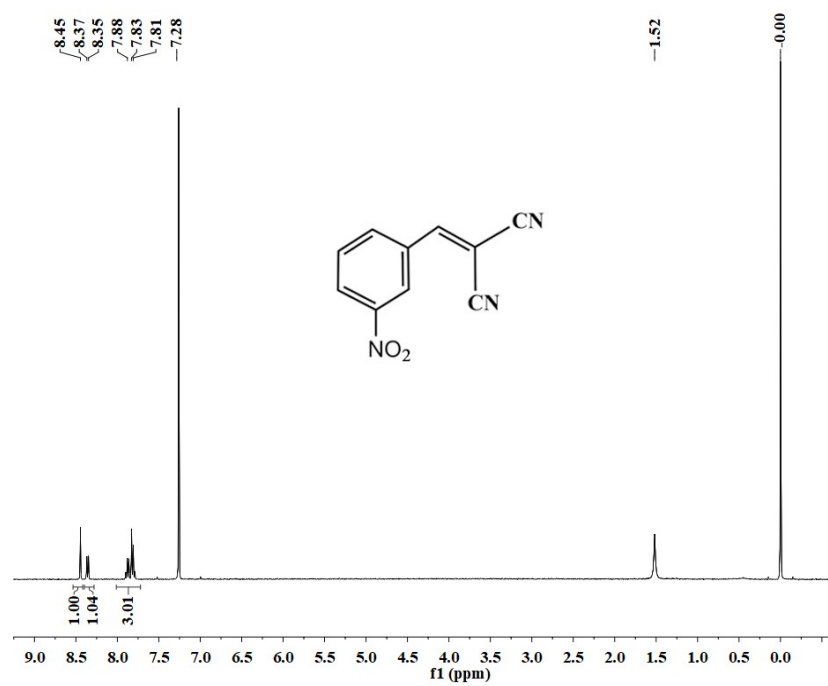


Figure S20 ^1H NMR spectra of 2-(3-nitrobenzylidene)malononitrile.

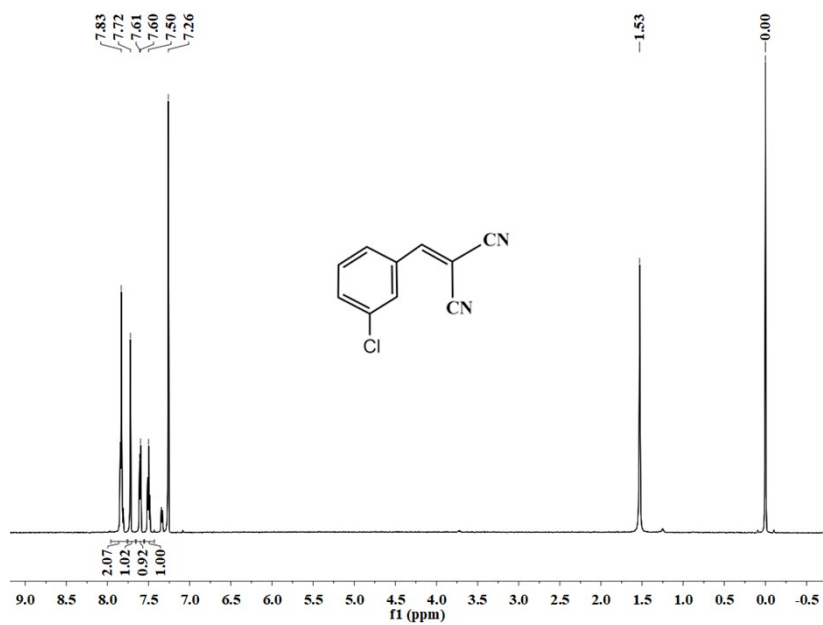


Figure S21 ^1H NMR spectra of 2-(3-chlorobenzylidene)malononitrile.

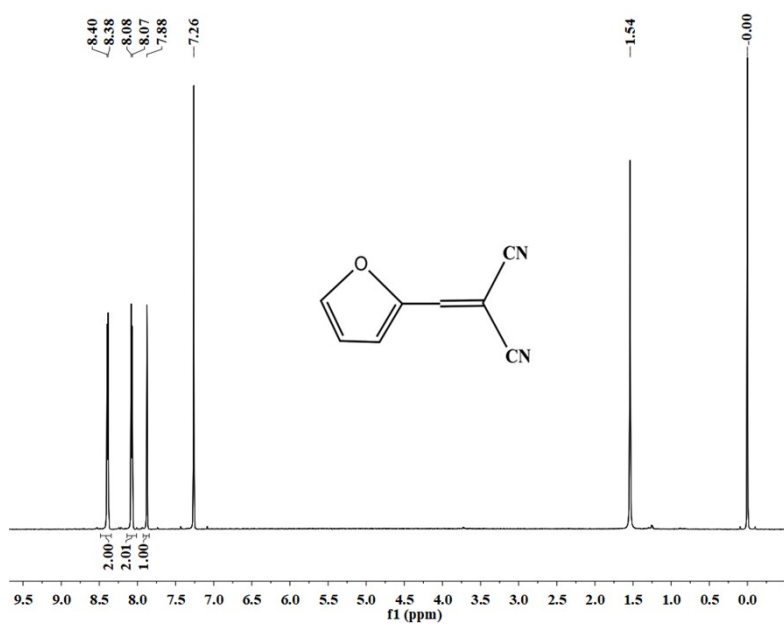


Figure S22 ^1H NMR spectra of 2-(furan-2-ylmethylene)malononitrile.



Figure S23 ^1H NMR spectra of 2-(4-methoxybenzylidene)malononitrile.

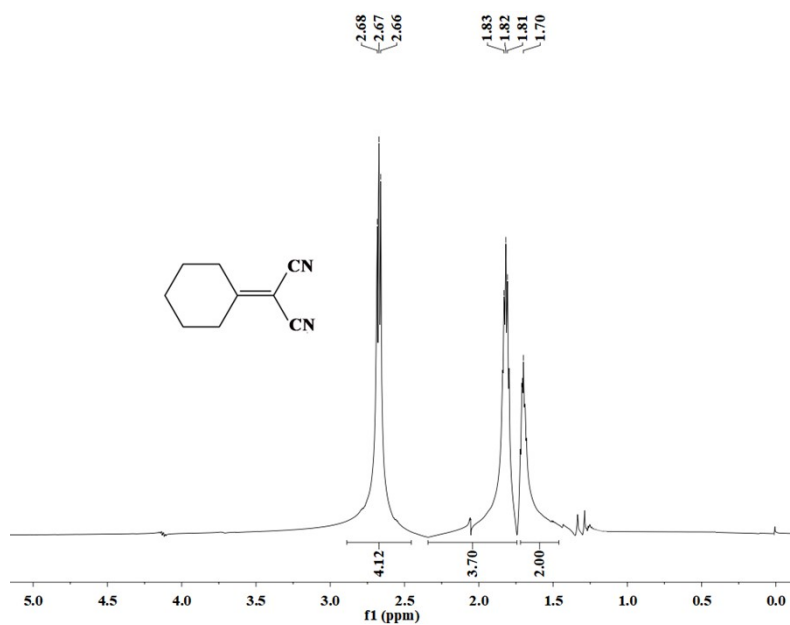


Figure S24 ^1H NMR spectra of 2-cyclohexylidenemalononitrile.

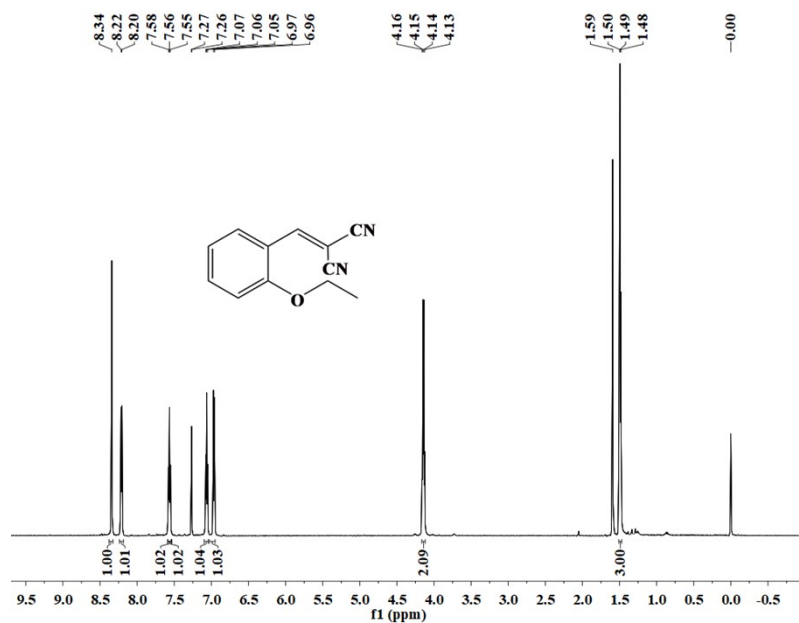


Figure S25 ^1H NMR spectra of 2-cyclohexylidenemalononitrile.

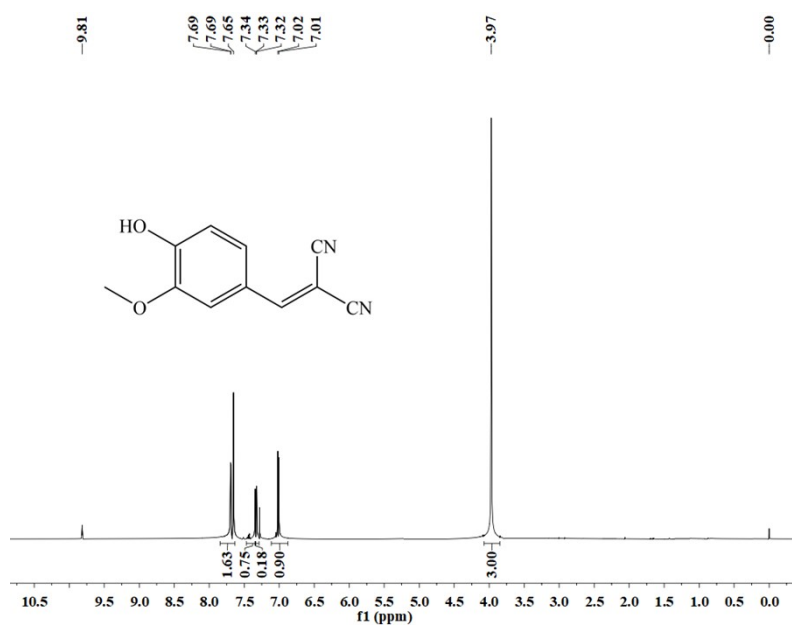


Figure S26 ^1H NMR spectra of 2-[(4-hydroxy-3-methoxyphenyl)methylidene]propanedinitrile.